Supporting Information for

The Interactions of Lipids and Detergents with a Viral Ion Channel Protein: Molecular Dynamics Simulation Studies.

Rouse, Sarah L. & Sansom, Mark S.P.

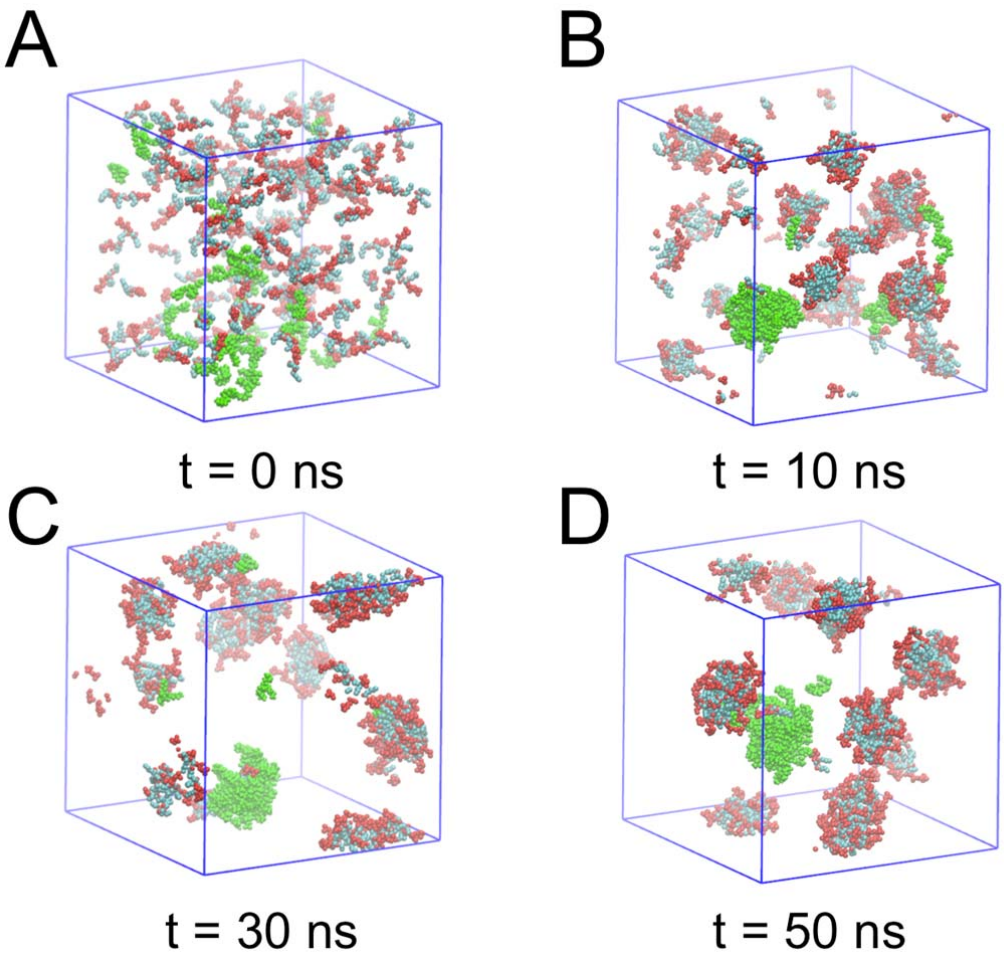

Figure S1 Snapshots showing self-assembly of DHPC monomers into micelles. A: The initial configuration of 200 randomly placed and orientated DHPC monomers. The system after B: 10ns, C: 30 ns and D: 50 ns. The phosphatidylcholine headgroups of DHPC are shown as red spheres, acyl tails are shown as cyan spheres. The detergent molecules coloured in green are those used in analysis of a single micelle (see text).

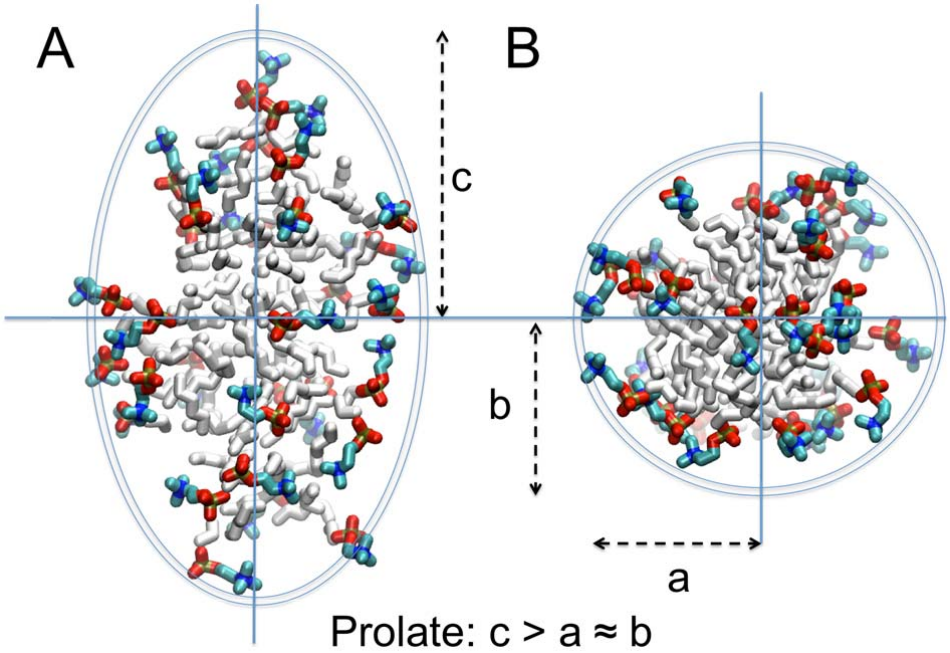

Figure S2 DHPC micelles are prolate. A: Side and B: top views of an individual DHPC micelle (N = 30). This micelle existed for ~ 75 ns of the 100 ns simulation. Blue lines indicate the axes of symmetry. Dashed black arrows indicate the semiaxis lengths.

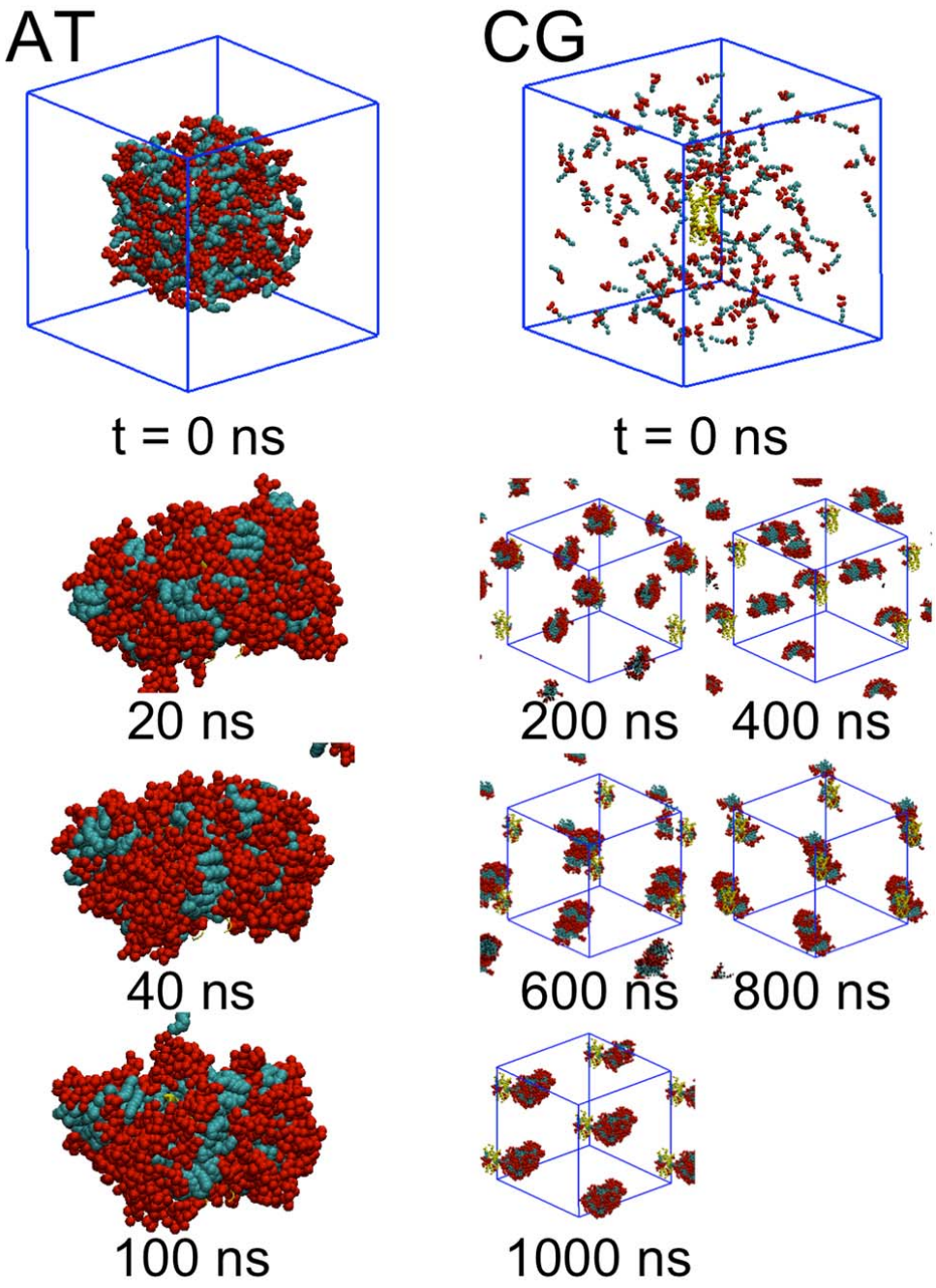

Figure S3 ATMD (left) and CGMD (right) simulations of DDM self-assembling around BM2. The AT simulation was biased to form a single protein detergent complex by adding the detergent molecules within a smaller box. The detergent does not rearrange to give a normal micelle (headgroups on the outside, hydrophobic tails sequestered on the inside) within the 100 ns timescale as evidenced by the snapshots shown. A CGMD simulation was performed from initially randomly placed DDM molecules. A normal micelle does not form during the 1 μs timescale, with detergent tails exposed to the solvent. Detergent headgroups are shown in red and tails in cyan. BM2 is coloured yellow. Solvent is omitted for clarity. The cubic box size was 10 $Å^3$ and 13.5 $Å^3$ for AT and CG simulations, respectively.

	N_{agg}	R_g	a (Å)	c (Å)	pl (Å)	a/c
Experiment [1]	25-35	20	9.5-10.0	20.5-22.5	3.0-4.0	2.2
MD (self-assembly)	30	15.6 (± 0.6)	16.6 (± 1.6)	24.3 (± 3.2)	3.7 (± 0.4)	1.5

Table S1. Properties of DHPC micelles calculated from experimental data [1] and from MD simulation. N_{agg} corresponds to the calculated aggregation number in experiment or the size of the micelle analyzed in the MD experiment. The radius of gyration is calculated using the program g_gyrate in GROMACS. Semiaxis lengths (a and c) and the polar length (pl) are calculated indirectly from the instantaneous moments of inertia (see text). All values from MD are the averages over the final 10 ns of the trajectory, with twice the standard deviation shown in parentheses.

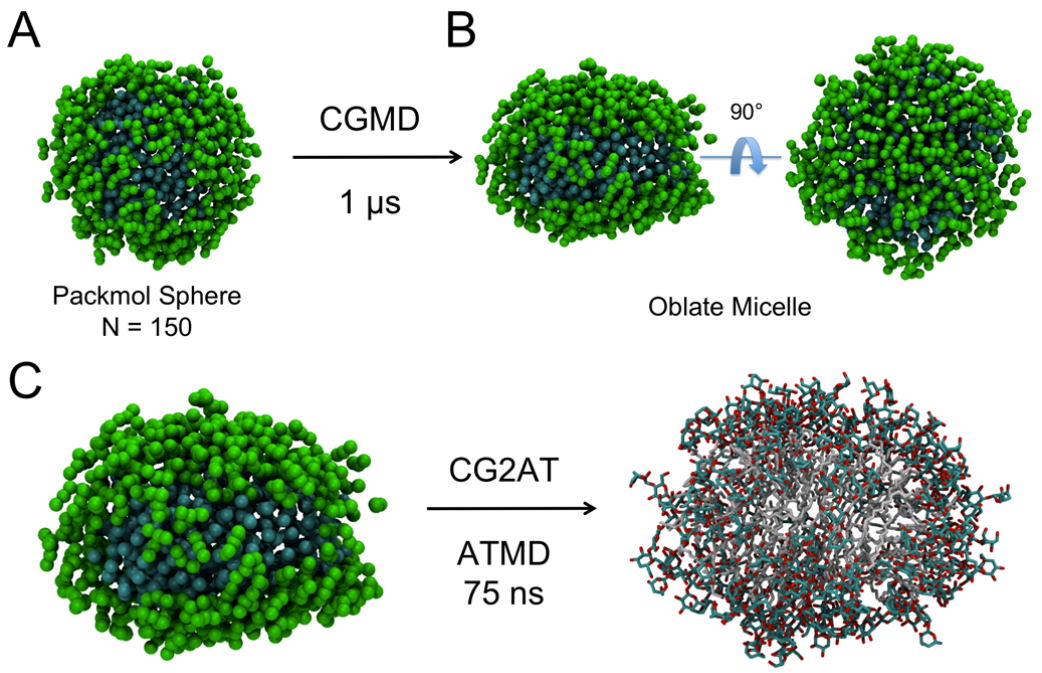

Figure S4. CGMD simulation of pre-formed DDM micelle. A: Initial spherical CG-DDM aggregate generated using the program Packmol. B: Side and top views of the DDM micelle following 1 μs of CGMD simulation. Maltose headgroups are shown as green spheres while the acyl tails are shown as cyan spheres. C: Conversion to atomistic (AT) representation and DDM micelle following a relatively long 75 ns ATMD simulation with the OPLS-AA force field. The micelle becomes more compact, while the oblate nature is retained. Acyl tails are shown in grey, headgroups are coloured according to atom type (red = oxygen, cyan = carbon). Hydrogen atoms and water molecules are omitted for clarity.

	N_{agg}	R_g (Å)	a (Å)	c (Å)	pl (Å)	a/c
Experiment [1]	135-145	33	28.0-29.5	13.8-14.3	6.0-6.3	0.48
MD [2]	132	25.2-26.4	37.2-38.8	26.5-30.1	7.2-7.7	0.71
OPLS-AA	132	24 (± 0.2)	33.1 (± 1.0)	28.4 (± 0.8)	7.1 (± 0.2)	0.86
GROMOS	150	24.9 (± 0.2)	34.0 (±1.0)	28.0 (±0.6)	5.1 (± 0.1)	0.82
OPLS-AA	150	24.4 (± 0.3)	34.2 (± 0.8)	27.2 (± 0.6)	7.1 (± 0.1)	0.79

Table S2. Properties of DDM micelles from experiment and molecular dynamics simulation. N_{agg} refers to the calculated aggregation number in the case of the experimental data, or the numbers of lipids chosen for the study in the case of MD work. R_g is the calculated radius of gyration of the detergent micelle. a and c correspond to the half-lengths of the secondary and principle axes of symmetry. pl corresponds to the length of the polar core (calculated as described previously in text). The ratio a/c gives and indication of the degree of ellipticity (tending towards one for a spherical aggregate).

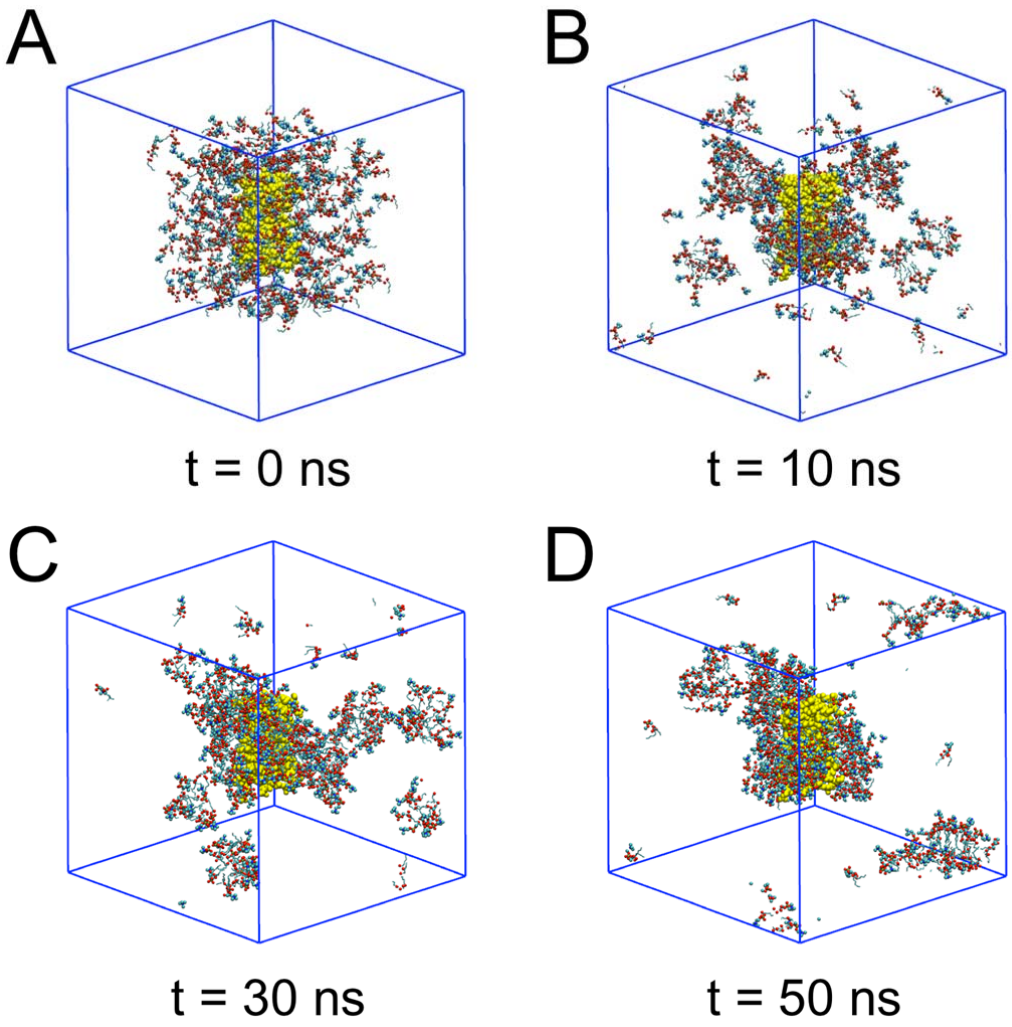

Figure S5. Self-assembly of BM2-DHPC complex. **A**: Starting point of simulation. Snapshots of the system at **B**: 10 ns, **C**: 30 ns and **D**: 50 ns. The phopshatidylcholine headgroups are shown as spheres (oxygen:red, carbon:cyan, nitrogen:blue, phosphorus:tan) and the carbon tails are shown as a cyan trace. The protein is shown as yellow spheres. Water is omitted for clarity.

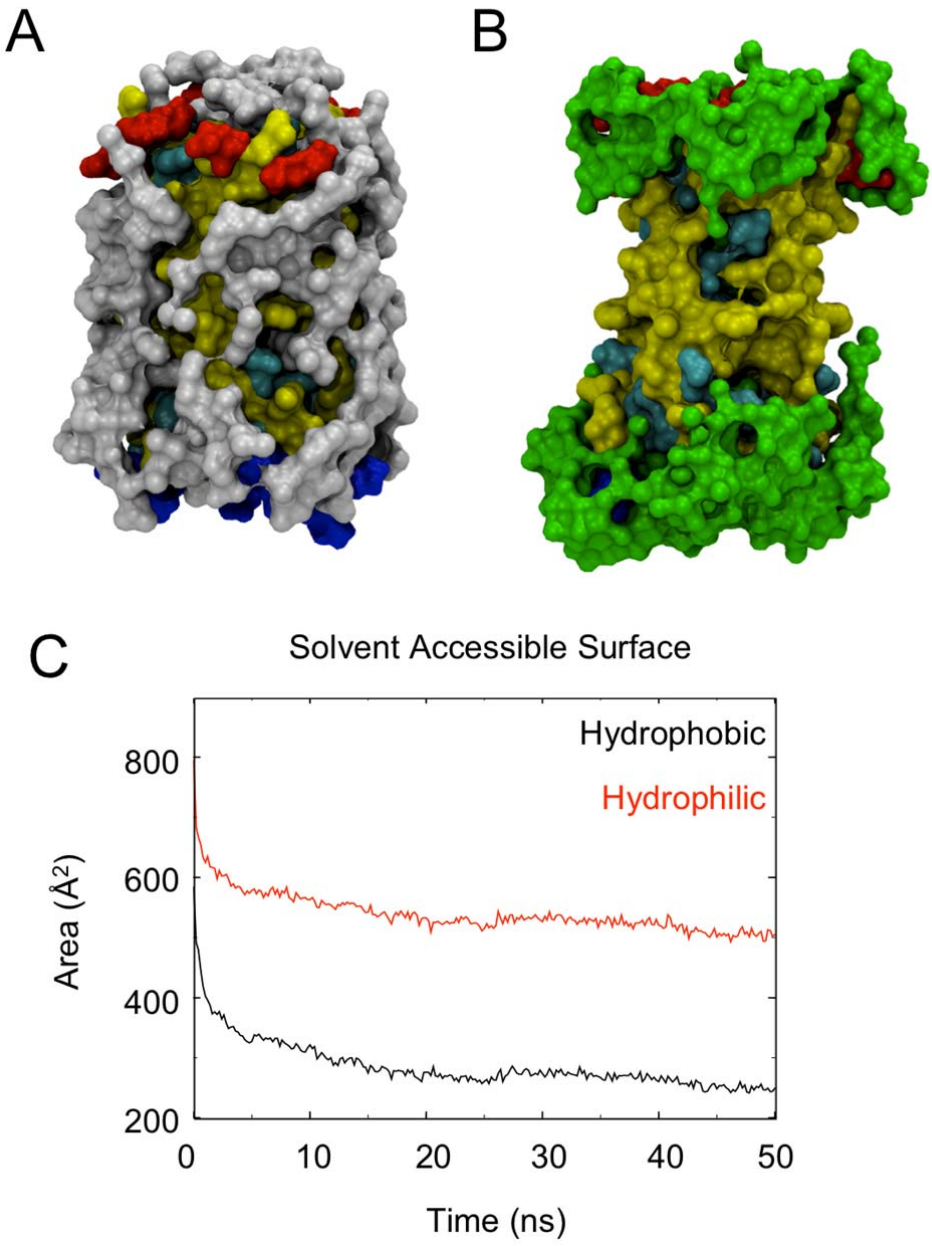

Figure S6. Solvent accessible surfaces of BM2. Top: protein surface after 50 ns coloured according to hydrophobicity of residues (red = negatively charged, blue = positively charged, cyan = polar, yellow = hydrophobic residues). **A**: DHPC atoms within 5 Å of the protein surface are shown as a grey surface. **B**: Water oxygen atoms within 5 Å of the protein surface are displayed as a green surface. **C**: Reduction in solvent accessible surface area of BM2 during initial 50 ns simulation. Surface areas of residues are classed as hydrophobic (black trace) and hydrophilic (red trace) based on partial charges (>0.2 corresponds to hydrophilic residue).

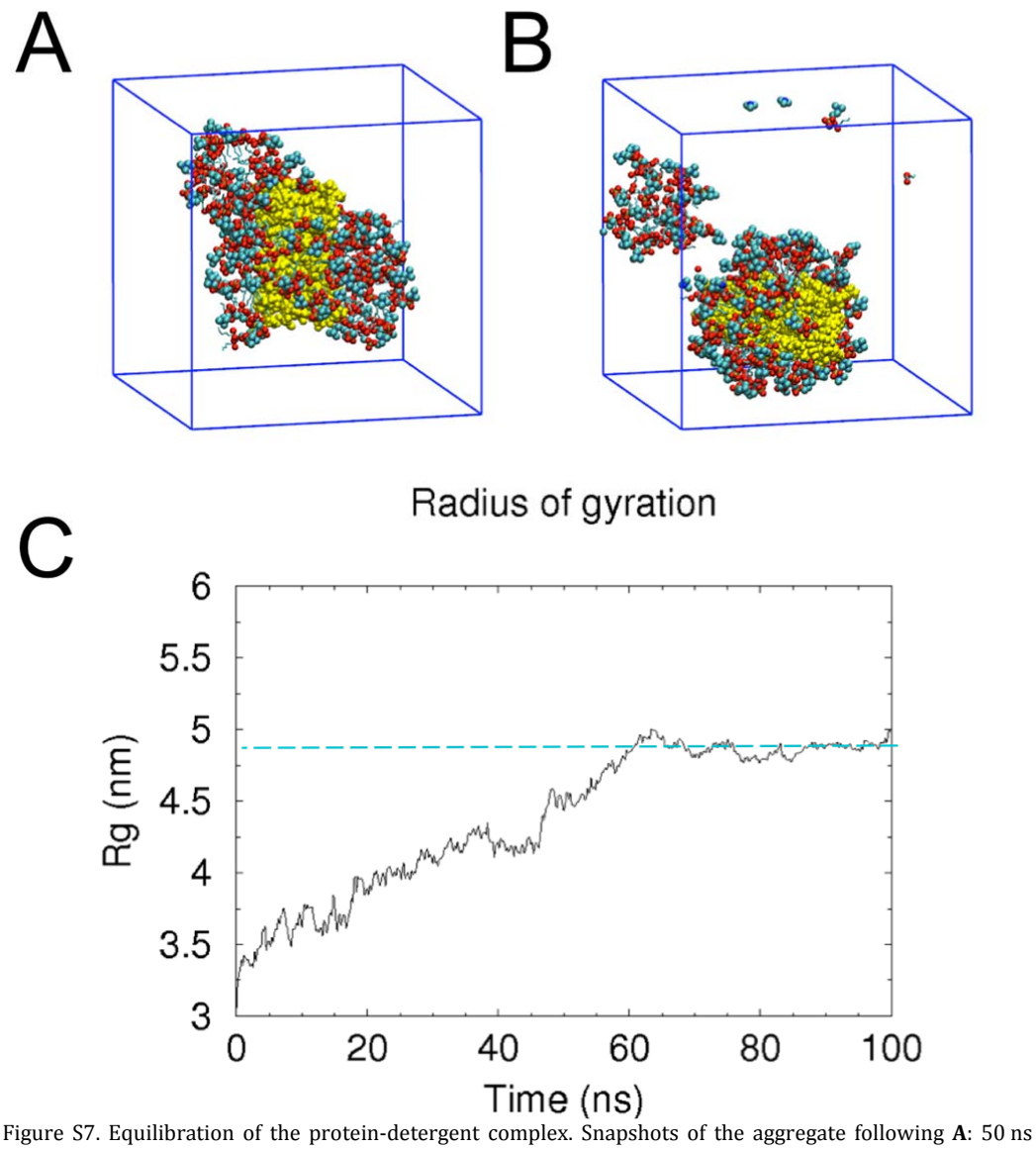

Figure S7. Equilibration of the protein-detergent complex. Snapshots of the aggregate following **A**: 50 ns self-assembly simulation and after **B**: 100 ns equilibration simulation. **C**: Calculated radius of gyration for those molecules in the final protein-detergent complex during 100 ns equilibration simulation. The dotted line in blue corresponds to the mean radius of gyration of the protein-detergent complex over the final 10 ns of the simulation.

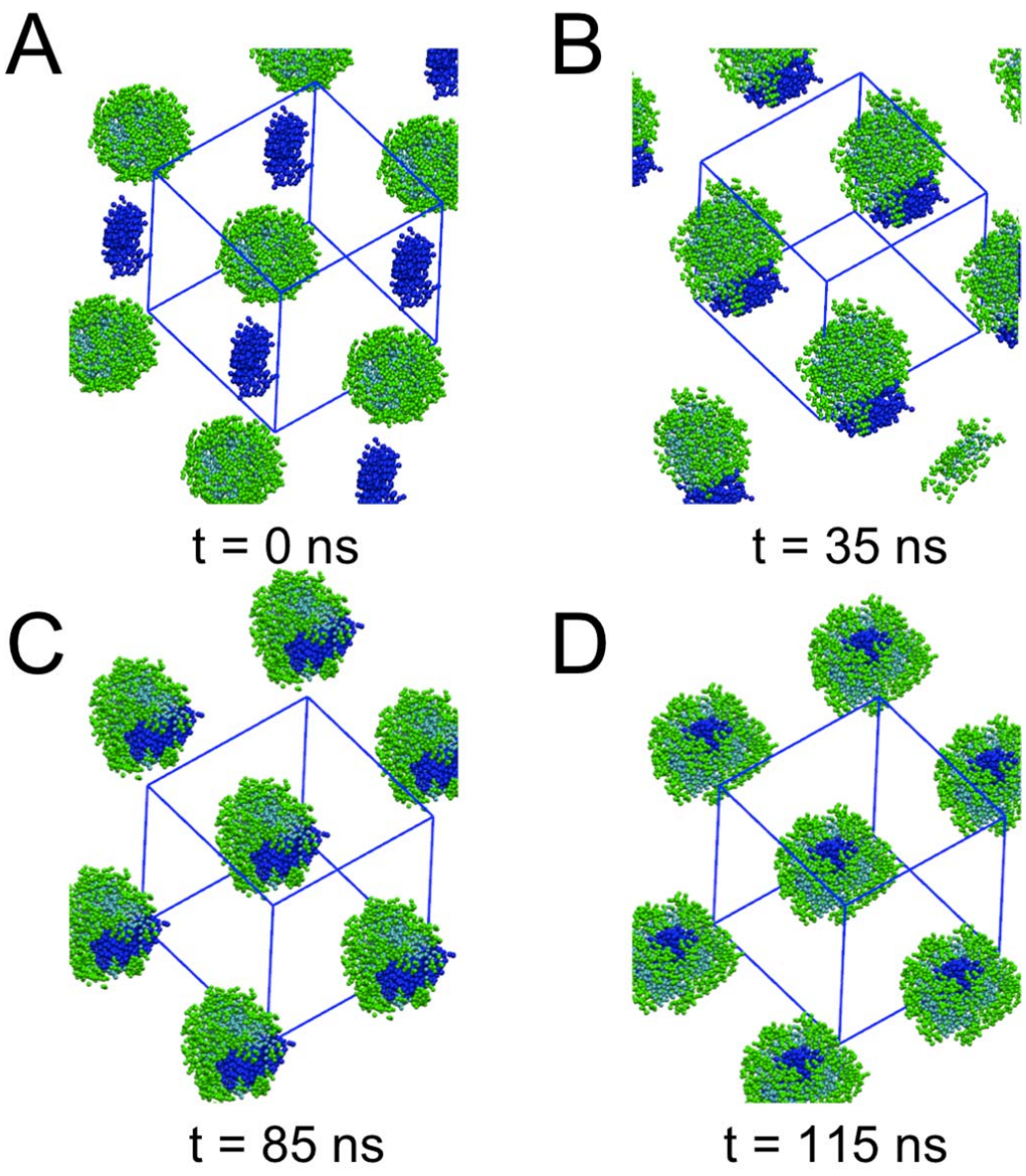

Figure S8. Snapshots of the BM2-DDM complex formation at **A**: 0 ns, **B**: 35 ns, **C**: 85 ns and **D**: 115 ns. The initial configuration has the BM2 and DDM micelle as far apart as possible. The protein rapidly contacts the DDM micelle and becomes incorporated into the centre of the micelle after 100 ns.. The simulation box is shown in blue, with periodic images in each dimension also shown.

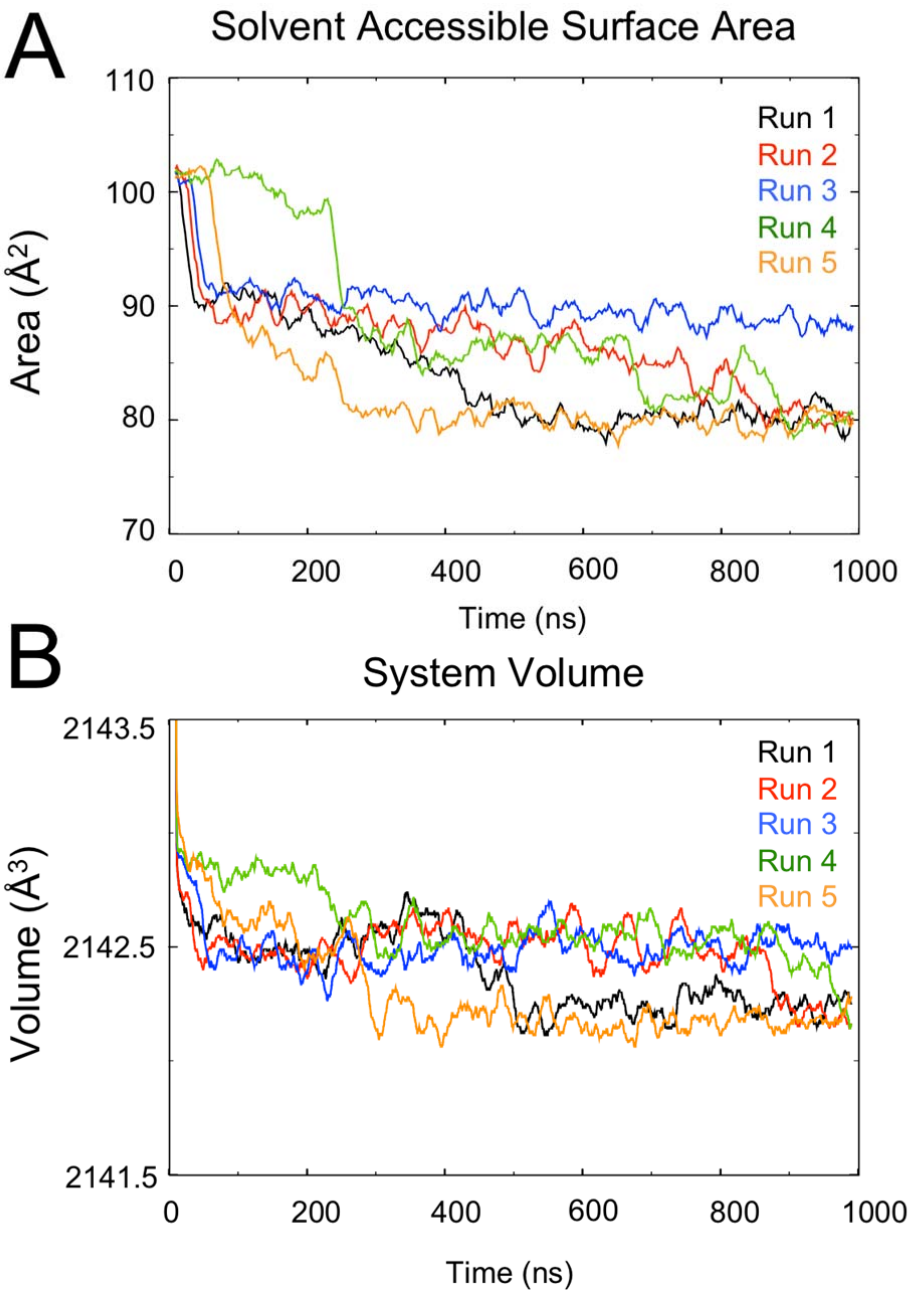

Figure S9. Properties of the system during BM2-DDM initial association and subsequent rearrangement. **A**: protein solvent accessible surface area (SASA) over time. **B**: system volume over time. The largest decrease in both SASA and volume is seen upon initial association with the DDM micelle. Data from each simulation is coloured according to plot legend. The data is shown as a running average over 100 data points.

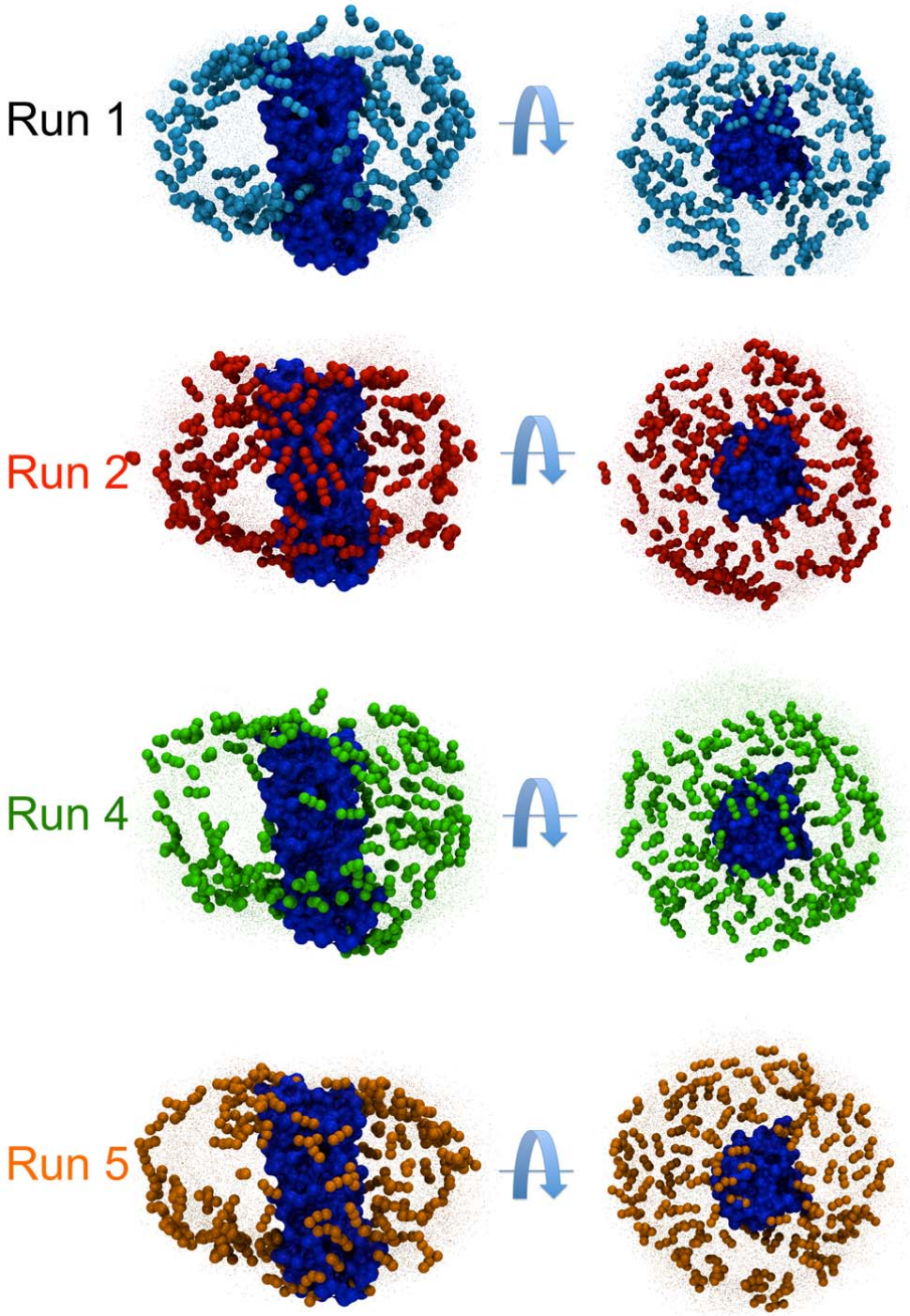

Figure S10. Final BM2-DDM complexes following 1μs CGMD simulation. The protein is shown as a blue surface. The most populated positions of the first ring of the maltose headgroups over the final 100 ns of CGMD simulation are shown spheres. The space sampled by the headgroups are shown by small dots. There is some evidence of headgroup clustering. Spatial distributions were calculated in the frame of reference of the protein.

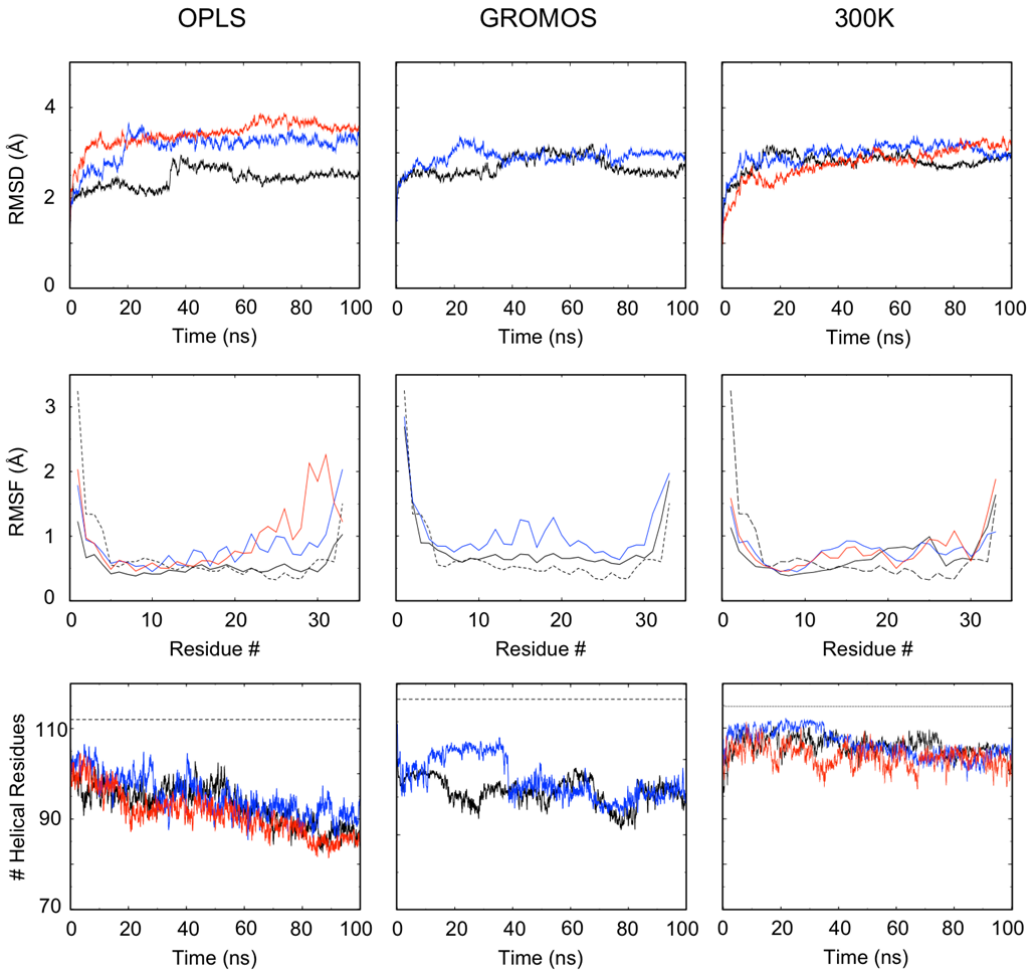

Figure S11. Simulations of BM2-TM in a DPPC bilayer. The OPLS force field was used at both 323 K ("OPLS|") and 300 K ("300K"). The gromos 56a3 ("GROMOS") force field was used at 323 K. Cα RMSDs (top panel), Cα RMS fluctuations (middle panel) and α-helical residue count (lower panel) for each simulation. RMSDs were calculated for all residues not including the 2 end residues at C- and N-termini. RMSFs are shown for the first chain only. The dashed line in the RMSF plots shows the Cα RMSD between the 15 structures deposited in the protein data bank. The dotted line in the secondary structure plots corresponds to the maximum α-helical count observed for the NMR structure with positional restraints maintained.

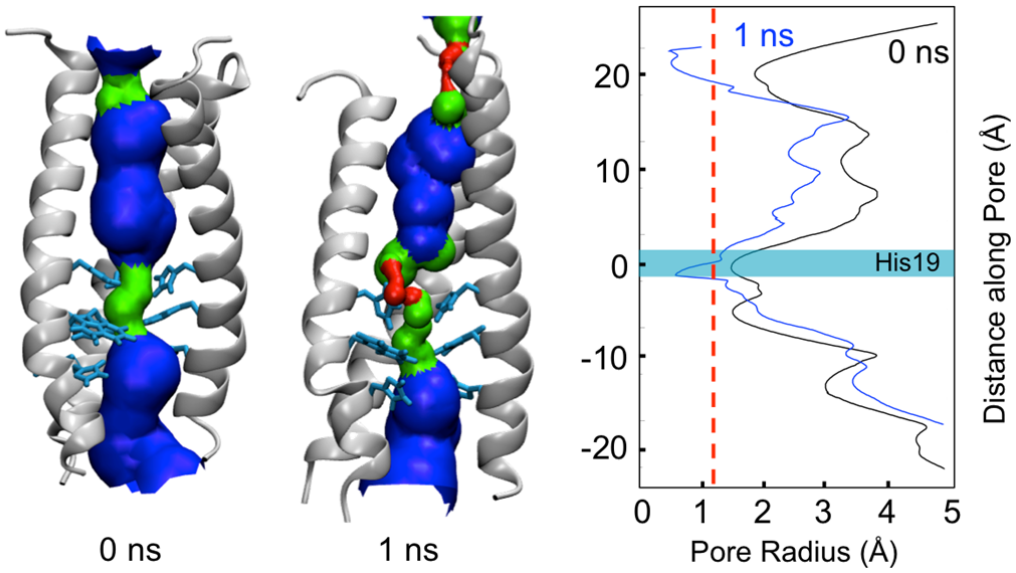

Figure S12. Collapse of the BM2-TM pore. Left: 3D representations of the pore surfaces of the BM2 NMR structure at beginning of simulation and after 1 ns using the OPLS force field. Profiles were calculated using HOLE.[3] The protein is shown as gray cartoon, with the front helix hidden for clarity. The His19, Trp23 and His27 residues are shown in cyan in a ball-and-sticks representation. The colours of the 3D profiles are as follows: red, radius < 1.2 Å (no water can pass); green, 1.2 Å ≤ radius ≤ 2.3 Å (single-file water); blue, radius > 2.3 Å (multiple waters may pass). The plot on the right shows the average pore radius relative to the His19 region. The approximate van der Waals radius of a water molecule is plotted as a red dashed line.

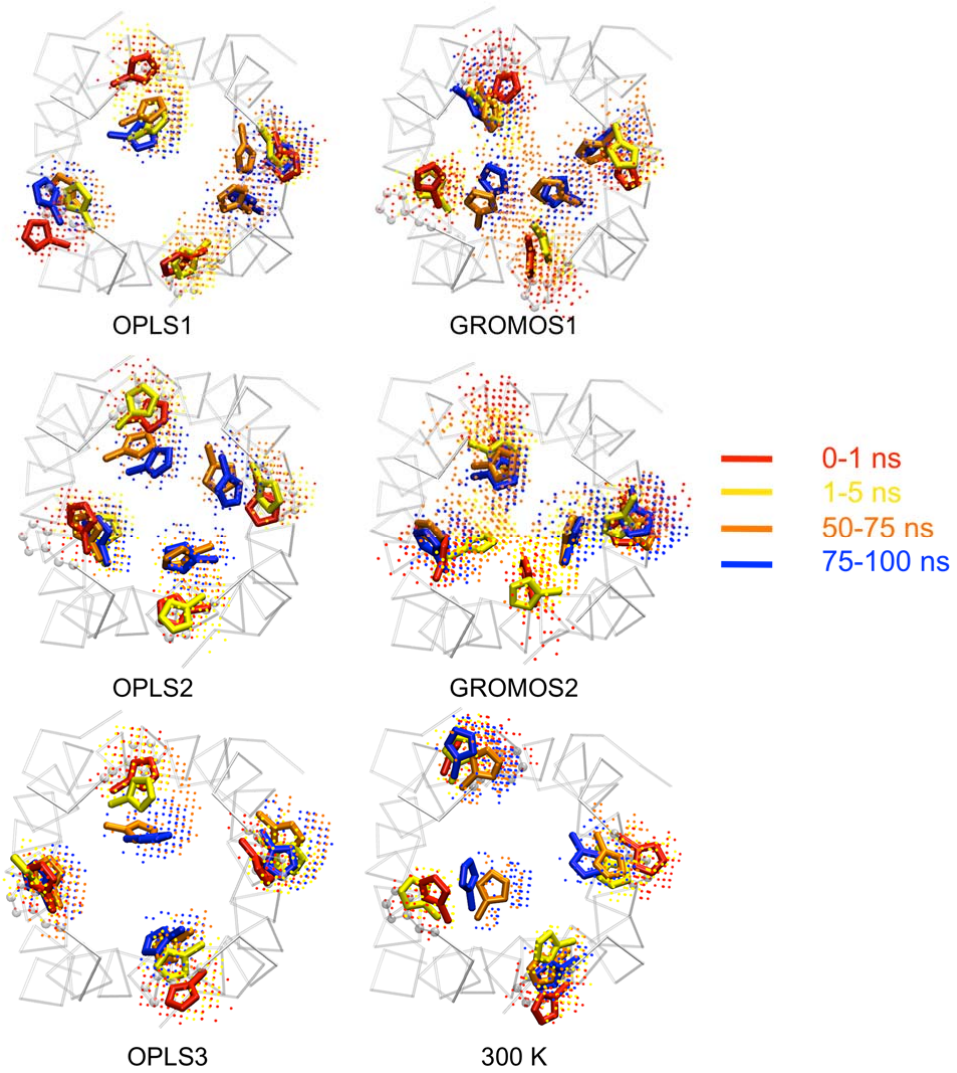

Figure S13. Rotation of His27 residues. Spatial distribution of His27 sidechains during 100 ns simulation. The helix backbones are shown as a thin grey trace with the initial orientation of His27 residues displayed in stick-and-ball representation. The space sampled by the His27 sidechains during each block of time is shown as dots, coloured as indicated. The average position of the His27 sidechain for each time is shown in stick representation.

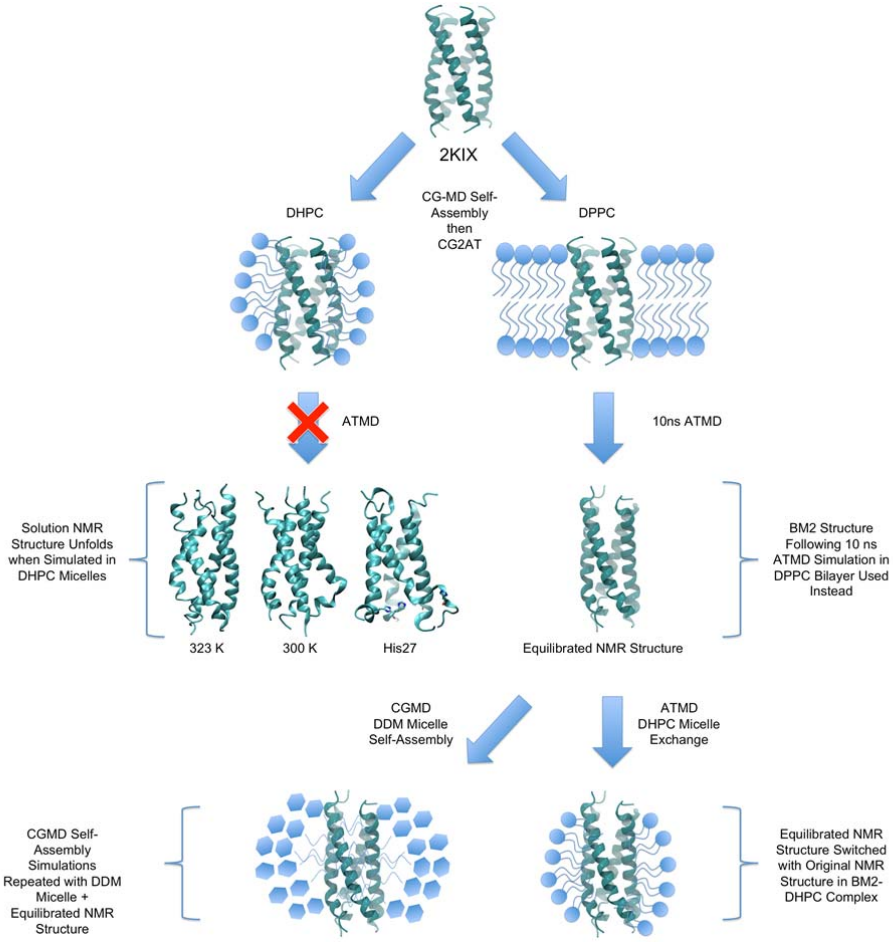

Figure S14. Equilibration of the solution NMR structure of the BM2 TM domain. Left: Snapshots of the solution NMR simulated in a DHPC micelle environment following i) 50 ns ATMD at 323 K ("323 K"), ii) 25 ns simulation at 300 K ("300 K "), iii) 100 ns simulation with all 4 histidine residues doubly-protonated at 323 K ("His27"). Unfolding and deviation from ideal helicity is observed in each case. Once 25 % of α-helical structure was lost the simulations were terminated. This occurred within 50 ns and 10 ns for the systems at 323 K and 300 K, respectively.

Right: The solution NMR structure following simulation at 323 K for 10 ns in a DPPC bilayer was used to generate new BM2-detergent complexes. For BM2-DHPC the initial NMR structure was replaced with the equilibrated one using the program g_membed [4]. This system was then simulated for 20 ns with positional restraints on the protein to allow the micelle to relax. The CGMD formation of DDM and BM2 was repeated using the equilibrated structure.

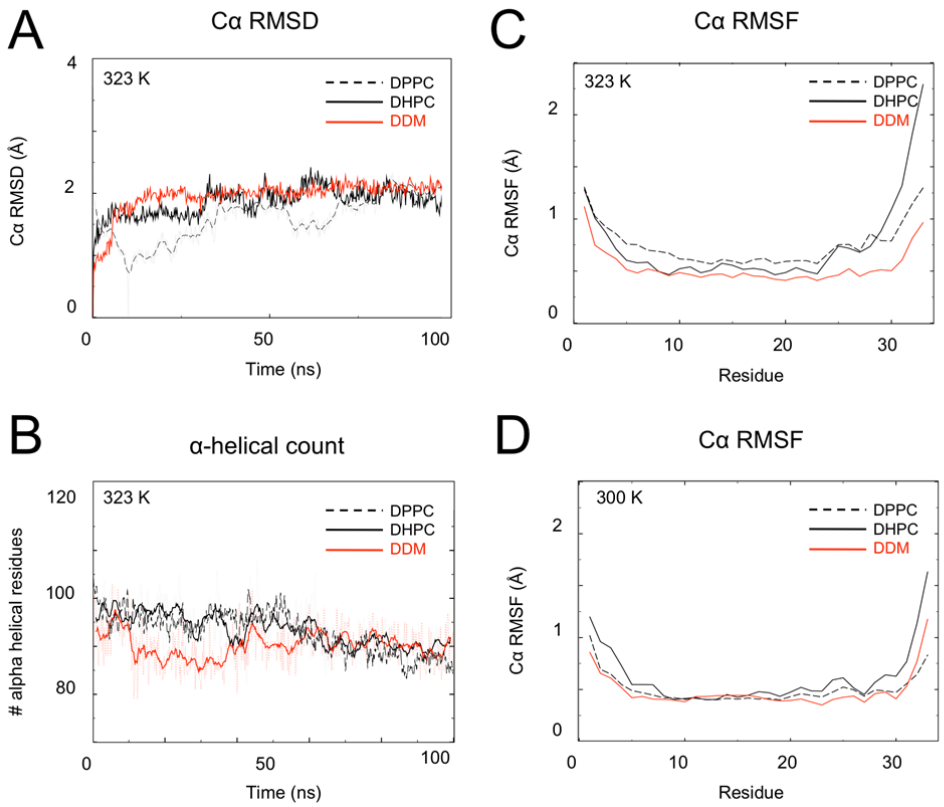

Figure S15. Stability and dynamics of the equilibrated NMR structure in different environments. **A**: Cα RMSD from the equilibrated micelle structure, not including the terminal 2 residues at each end. **B**: α-helical count during 100 ns simulation. **C**: The RMS fluctuation of Cα particles during the final 10 ns of simulation at 323 K, averaged over the 4 chains. **D**: As for C, but for simulations at 300 K. The black dashed trace corresponds to DPPC bilayer simulations, the black solid trace corresponds to DHPC micelle simulations, and the red line corresponds to DDM simulations, as indicated in the figure legends.

Detergent	Temperature (K)	Cα RMSD (Å)	α-helical Count (Number of Residues)	Maximum Bending Angle in Degrees
DHPC	323	1.8	90	32
DHPC	323	2.2	89	57
DHPC	323	1.7	100	51
DHPC	300	1.4	97	36
DDM	323	2.1	90	52
DDM	323	2.7	92	52
DDM	323	2.7	93	42
DDM	300	2.0	89	41

Table S3 Details of protein stability during simulations. The Cα RMSD corresponds to the deviation between structures at 0 and 100 ns of simulation. The number of residues in an α-helical conformation averaged over the final 10 ns is shown. The maximum bending angle in the structure at 100 ns is shown, calculated using Bendix [5]

Protein	Detergent	a	b	c	a/c
No	DHPC	1.66	1.92	2.43	1.46
Yes	DHPC	2.48	2.69	3.10	1.25
No	DDM	3.42	3.04	2.72	0.79
Yes	DDM	3.91	3.29	2.84	0.73

Table S4 Protein-detergent complexes retain geometry of parent micelles. Semiaxis lengths (a and c) and ellipticity ratios of DHPC and DDM micelles with and without BM2 present. These were calculated from the instantaneous moments of inertia over the final 10 ns of each simulation at 323 K (see text).

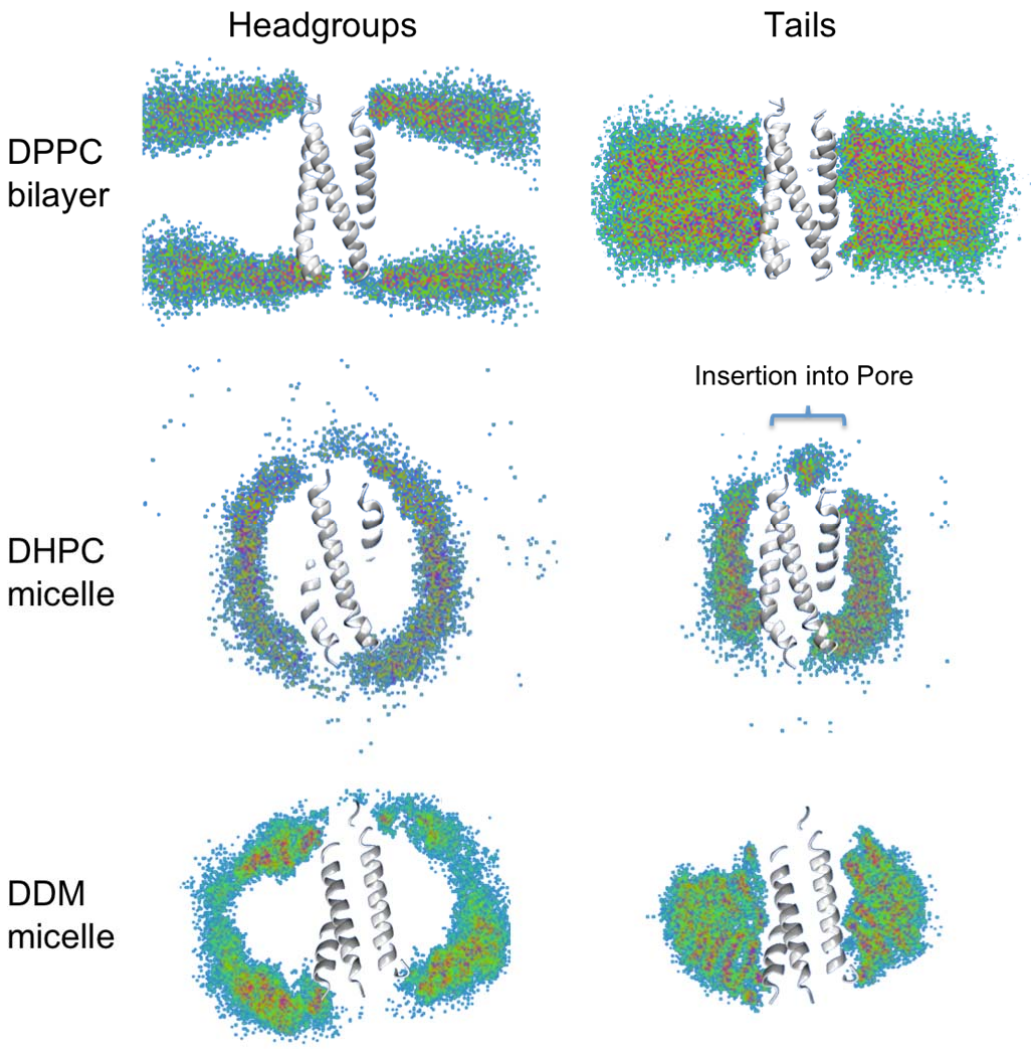

Figure S16. Spatial distributions of lipid/detergent headgroups and tails. Volume slices through protein centre of mass are shown. These were calculated over the last 50 ns of simulation, in the reference frame of the protein. Red regions correspond to high density throughout simulation and blue regions correspond to lowest occupancy.

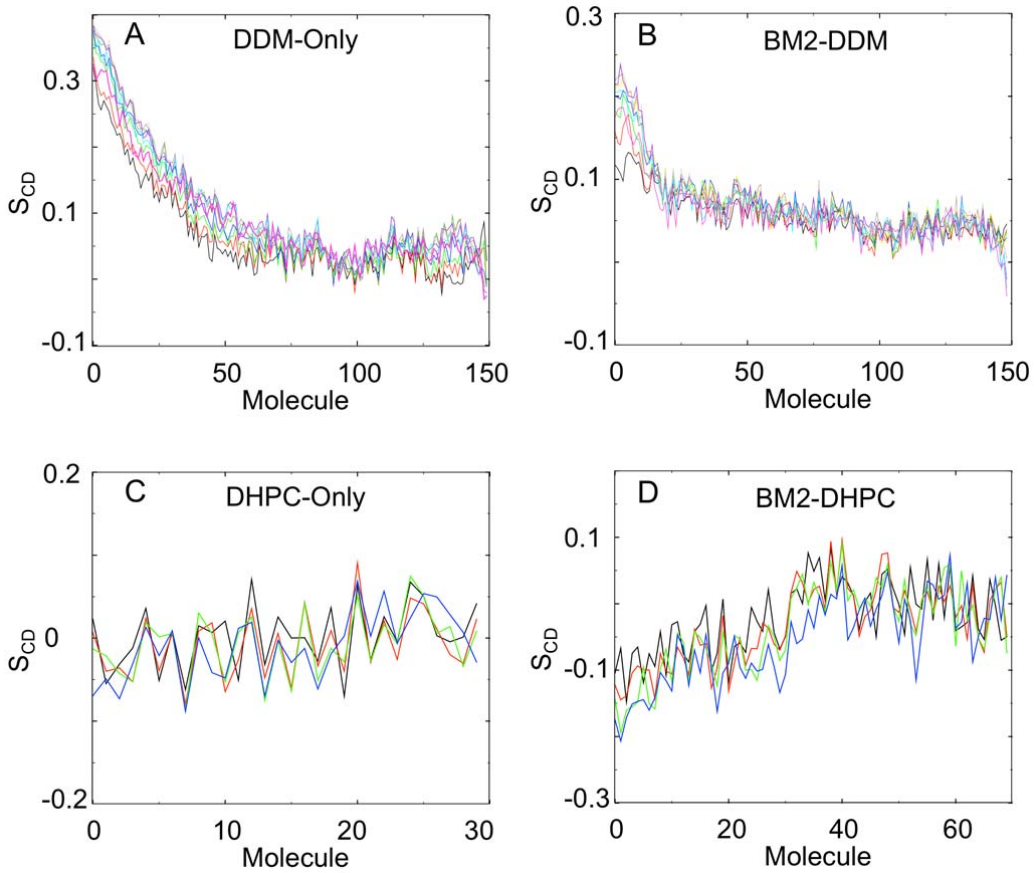

Figure S17. DDM and DHPC acyl chain order parameters S_{CD}. The order parameter S_{CD} may be used as a measure of alignment along the z-direction [6], in this case the principal axis of the protein, as a function of distance from the BM2-TM centre of mass. A value of 1 implies parallel orientation, -0.5 corresponds to a perpendicular orientation and zero means there is no overall alignment. **A,B**: the DDM N=150 system and **C,D**: the BM2-DHPC systems. The trajectories were renumbered such that the lipids were ordered in terms of the distance from the protein centre of mass for each frame., such that molecule 1 refers to the DDM lipid that is closest to the protein in a given frame of the trajectory and does not necessarily correspond to the same detergent molecule over time. The S_{CD} order parameter may then be calculated as a function of distance from the protein centre of mass. This parameter corresponds to the alignment of the detergent tails relative to the principle axis of the helix bundle.

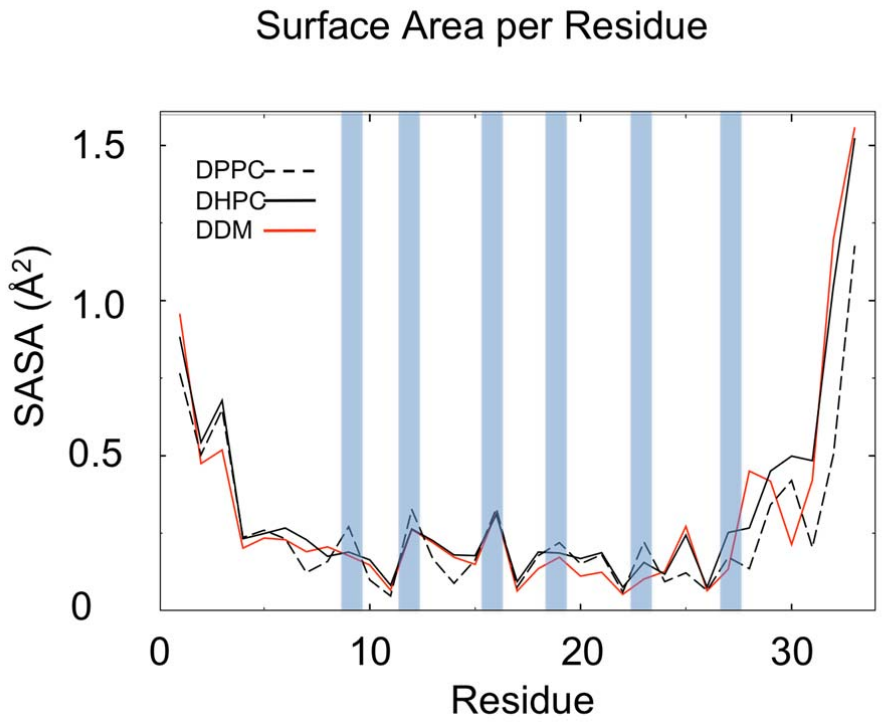

Figure S18. Averaged solvent accessible surface area over chain and last 10ns of each simulation. The DPPC simulation is shown as a black dashed line, the solid black line indicates the DHPC simulation and the red line corresponds to the DDM simulations. Blue bars indicate pore-lining residues.

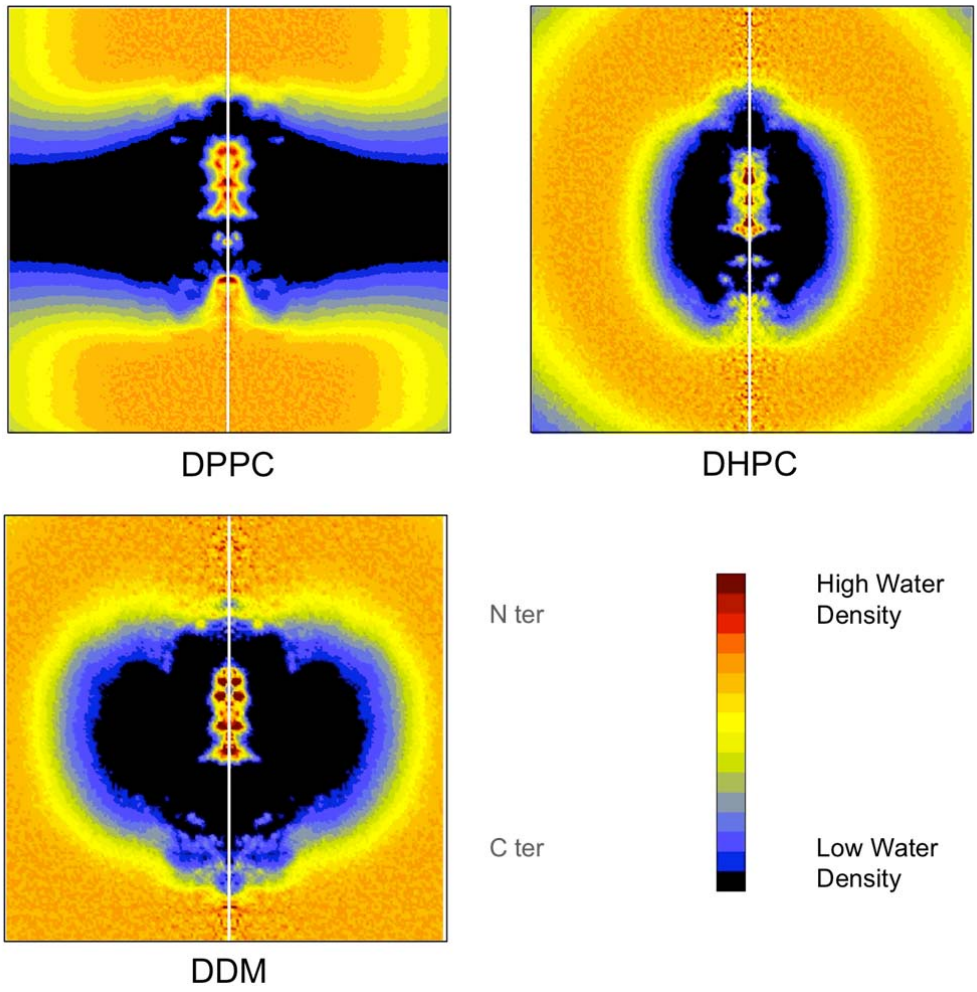

Figure S19. Radial density plots of water. Water densities relative to bulk water were calculated with gridcount. Radial distributions of water molecules are averaged over 100 ns simulation in a DPPC bilayer, DHPC micelle and DDM micelle. The axis of the BM2 tetramer is indicated by a white line. Water density is observed within the pore of the channel. The N terminal region is at the top of the plot as indicated by the N ter and C ter labels.

Additional references

(1) Lipfert, J.; Columbus, L.; Chu, V. B.; Lesley, S. A.; Doniach, S. Size and Shape of Detergent Micelles Determined by Small-Angle X-Ray Scattering. *J. Phys. Chem. B* **2007**, *111*, 12427–12438.

(2) Abel, S.; Dupradeau, F.-Y.; Raman, E. P.; MacKerell, A. D.; Marchi, M. Molecular Simulations of Dodecyl-B-Maltoside Micelles in Water: Influence of the Headgroup Conformation and Force Field Parameters. *J. Phys. Chem. B* **2011**, *115*, 487–499.

(3) Smart, O. S.; Neduvelil, J. G.; Wang, X.; Wallace, B. A.; Sansom, M. S. HOLE: A Program for the Analysis of the Pore Dimensions of Ion Channel Structural Models. *J. Mol. Graph.* **1996**, *14*, 354–360, 376.

(4) Wolf, M. G.; Hoefling, M.; Aponte-Santamaría, C.; Grubmüller, H.; Groenhof, G. G_membed: Efficient Insertion of a Membrane Protein into an Equilibrated Lipid Bilayer with Minimal Perturbation. *J. Comput. Chem.* **2010**, *31*, 2169–2174.

(5) Dahl, A. C. E.; Chavent, M.; Sansom, M. S. P. Bendix: Intuitive Helix Geometry Analysis and Abstraction. *Bioinformatics* **2012**, *28*, 2193–2194.

(6) Leach, A. Molecular Modelling: Principles and Applications. **2001**.